Histol Histopathol (2020) 35: 1415-1426

http://www.hh.um.es

Histology and Histopathology
From Cell Biology to Tissue Engineering

Proliferative and chondrogenic potential of mesenchymal stromal cells from pluripotent and bone marrow cells

Irene Sfougataki[1,2], Ioanna Varela[1], Kalliope Stefanaki[3], Angeliki Karagiannidou[1], Maria G. Roubelakis[4], Vasiliki Kalodimou[5], Ioanna Papathanasiou[6], Joanne Traeger-Synodinos[7], Sofia Kitsiou-Tzeli[7], Emmanuel Kanavakis[8], Vasiliki Kitra[1], Aspasia Tsezou[6], Maria Tzetis[7] and Evgenios Goussetis[1]

[1]Stem Cell Transplant Unit, Aghia Sophia Children's Hospital, [2]Research Institute for the Study of Genetic and Malignant Disorders in Childhood, Aghia Sophia Children's Hospital, [3]Department of Histopathology, Aghia Sophia Children's Hospital, [4]Laboratory of Biology, Medical School, National and Kapodistrian University of Athens, [5]Flow Cytometry-Research and Regenerative Medicine Department, IASO Hospital, Athens, [6]Laboratory of Cytogenetics and Molecular Genetics, Faculty of Medicine, University of Thessally, Thessally, [7]Department of Medical Genetics, Medical School, National and Kapodistrian University of Athens, Athens and [8]Genesis Genoma Lab, Genetic diagnosis, Clinical Genetics and Research, Chalandri, Greece

Summary. Introduction. Mesenchymal stromal cells (MSCs) can be derived from a wide range of fetal and adult sources including pluripotent stem cells (PSCs). The properties of PSC-derived MSCs need to be fully characterized, in order to evaluate the feasibility of their use in clinical applications. PSC-MSC proliferation and differentiation potential in comparison with bone marrow (BM)-MSCs is still under investigation. The objective of this study was to determine the proliferative and chondrogenic capabilities of both human induced pluripotent stem cell (hiPSC-) and embryonic stem cell (hESC-) derived MSCs, by comparing them with BM-MSCs.

Methods. MSCs were derived from two hiPSC lines (hiPSC-MSCs), the well characterized Hues9 hESC line (hESC-MSCs) and BM from two healthy donors (BM-MSCs). Proliferation potential was investigated using appropriate culture conditions, with serial passaging, until cells entered into senescence. Differentiation potential to cartilage was examined after *in vitro* chondrogenic culture conditions.

Results. BM-MSCs revealed a fold expansion of $1.18x10^5$ and $2.3x10^5$ while the two hiPSC-MSC lines and hESC-MSC showed $5.88x10^{10}$, $3.49x10^8$ and $2.88x10^8$, respectively. Under chondrogenic conditions, all MSC lines showed a degree of chondrogenesis. However, when we examined the formed chondrocyte micromasses by histological analysis of the cartilage morphology and immunohistochemistry for the chondrocyte specific markers Sox9 and Collagen II, we observed that PSC-derived MSC lines had formed pink rather than hyaline cartilage, in contrast to BM-MSCs.

Conclusion. In conclusion, MSCs derived from both hESCs and hiPSCs had superior proliferative capacity compared to BM-MSCs, but they were inefficient in their ability to form hyaline cartilage.

Key words: Mesenchymal Stromal Cells, Pluripotent Stem Cells, Bone Marrow, Cell Proliferation, Chondrogenesis

Offprint requests to: Irene Sfougataki, PhD, Stem Cell Transplant Unit, Aghia Sophia Children's Hospital, Levadias 8, 11527 Athens, Greece. e-mail : irene_sf_@hotmail.com

DOI: 10.14670/HH-18-259

Introduction

Mesenchymal stromal cells (MSCs) have been, intensely investigated during the last years in multiple studies, for their possible usage in cellular therapy due to their unique biological characteristics. MSCs represent multipotent adult stem cells that exhibit several *in vitro* properties, including adherence to plastic surface, ability to proliferate, specific antigen expression ($CD73^+$

$CD90^+$ $CD105^+$ $CD34^-$ $CD11b^-$ $CD14^-$ $CD19^-$ $HLADR^-$) and ability to generate osteoblasts, adipocytes and chondrocytes, upon culture in appropriate conditions (Dominici et al., 2006; Wang et al., 2012; Sharma et al., 2014). Research has focused on their differentiation and immunomodulatory abilities, as well as in their trophic role in tissue repair by secretion of pro-angiogenic and growth factors into the damaged area. Their beneficial role has been observed in clinical studies regarding cardiac ischemic disease (Wang et al., 2012), acute graft versus host disease (Sharma et al., 2014) and other inflammatory, ischemic and autoimmune disorders, like Crohn's disease (Murphy et al., 2013). Osteoarthritis (OA) is one of the most common degenerative joint diseases without effective therapy so far and there is need for the establishment of alternative strategies of therapy. Cellular therapy using MSCs and MSC-derived chondrocytes could possibly provide reparative results, as indicated by several studies (Nejadnik et al., 2010; Toh, 2016).

MSCs are found in numerous adult tissues including bone marrow (BM), dental pulp, adipose tissue, muscle and other connective tissues, as well as in several fetal tissues, such as umbilical cord, cord blood, placenta and amniotic fluid (Hass et al., 2011). The most common source for MSC isolation, used in preclinical and clinical studies, is the BM (Sabapathy and Kumar, 2016). However, MSCs are represented in low numbers in BM (Hass et al., 2011) and they can be *in vitro* expanded only to a limited extent, as they display senescence after a few passages (Sabapathy and Kumar, 2016), resulting in insufficient numbers of healthy MSCs for cellular therapy. Furthermore, derivation of MSCs from adult tissues usually requires invasive procedures (Hass et al., 2011). Several groups have already reported the generation of MSCs from human embryonic stem cells (hESCs) and induced pluripotent stem cells (hiPSCs) with high yields (Chen et al., 2012; Liu et al., 2012; Villa-Diaz et al., 2012; Wei et al., 2012; Hynes et al., 2014; Tang et al., 2014), presenting a new source of these cells, which has unlimited capacity of expansion and differentiation. Pluripotent stem cell (PSC-) derived MSCs (PSC-MSCs) have been shown to resemble the phenotypical characteristics of adult MSCs and seem to have similar functional characteristics to BM-MSCs, such as inhibitory activity upon NK cells, by impeding their proliferation and cytotoxic potential *in vitro* (Giuliani et al., 2011). *In vivo* properties of PSC-derived MSCs have also been documented by preliminary results, showing that they are capable of engrafting onto injured murine muscle (Awaya et al., 2012), have regenerative potential in mice with hind limb ischemia (Lian et al., 2010) and exhibit the capacity to generate bone in mice with calvarian and radial defects (Villa-Diaz et al., 2012; Sheyn et al., 2016). In the present study, MSCs derived from two hiPSC lines and the well characterized Hues9 hESC line were examined for their proliferative capacity as well as for their chondrogenic capacity in comparison with BM-MSCs.

Materials and methods

Pluripotent cell lines

The protocol of the current study was approved by the Ethical Committee of Aghia Sophia Children's Hospital in Athens, Greece. Bone marrow samples were derived from the iliac crest of two normal 6 and 13 year-old stem cell transplant donors and 15 ml of each were used for the isolation of MSCs (BM-1-MSCs and BM-2-MSCs, respectively). Written informed consent was provided from the parents. After harvesting, bone marrow MSCs (BM-MSCs) were isolated from the mononuclear cell layer, according to standard protocols (Varela et al., 2014) and cultured in Dulbecco's Modified Eagle Medium (DMEM) with Glutamax (Gibco, BRL) containing 10% Fetal Bovine Serum (FBS) (Stem Cell Technologies, Vancouver, BC, Canada). An amount of $25x10^3$ cells from both BM-MSC lines was subsequently used to generate hiPSCs and the remaining cells were stored in liquid nitrogen. For the reprogramming, a modified synthetic mRNA method (Warren et al., 2010) (Stemgent, Cambridge, MA, USA) was used, as previously described (Varela et al., 2014). After establishment of the hiPSC lines, two of them, hiPSC-1 and hiPSC-2 (one obtained from each initial BM sample) were used for the experiments. Pluripotent stem cells (PSCs) were cultured in standard culture conditions, in 6-well plates precoated with Matrigel hESC-qualified Matrix (BD Bioscience, Franklin Lakes, NJ, USA), containing mTeSR1 medium (Stem Cell Technologies, Vancouver, BC, Canada). Cells were fed every day with fresh medium and were passaged every 4-7 days, after enzymatic treatment with Dispase 1 U/ml (Stem Cell Technologies) for 1 minute and subsequent manual scraping of colonies. Expression of pluripotency genes in the hiPSC lines was confirmed as previously described (Varela et al., 2014). For comparative assessment of hiPSC and hESC derivatives, Hues9 hESCs line, kindly provided by Professor D. Melton, Harvard Stem Cell Institute, was similarly cultured and used in the experiments.

In vivo teratoma formation and tumor generation assays

Each undifferentiated hiPSC line was tested prior to mesenchymal differentiation (passage 20) with *in vivo* experiments for functional pluripotency. After mesenchymal differentiation and expansion (passage 4) each hiPSC-MSC line was examined *in vivo* for tumor generation. Approximately $1x10^6$ hiPSCs or hiPSC-derived MSCs were suspended in 100 μl of DMEM/F-12 (Stem Cell Technologies) mixed with Matrigel at a ratio 1:1 and were then delivered into three NOD/SCID mice, with subcutaneous administration. The animal experiments were carried out at the Animal Facility of the Biomedical Research Foundation of the Academy of Athens (BRFAA), in accordance with the directions of the Association for Assessment and Accreditation of

Laboratory Animal Care (AAALAC) and the recommendations of the Federation of European Laboratory Animal Science Associations (FELASA). After approximately 2-2.5 months, animals were sacrificed and tumors were collected. After fixation in 4% formaldehyde, processing in paraffin and sectioning, hematoxylin and eosin (H&E) staining was used to histologically assess the formed tissues.

Differentiation of pluripotent stem cells into mesenchymal stromal cells and expansion

The two hiPSCs lines (hiPSC-1, hiPSC-2) and Hues9 were induced towards the mesenchymal lineage via embryoid body (EB) formation, as previously described (Karagiannidou et al., 2014). Briefly, undifferentiated PSCs were cultured as aggregates in ultra-low attachment plates, in medium containing Knockout DMEM, 20% Knockout serum replacement (KSR), 1 mM L-Glutamine, 1x non-essential amino acids, 0.1 mM 2-mercaptethanol (all from Gibco) and 50 ng/ml BMP-4 (R&D System, Inc., Minneapolis, MN). After 7 days, embryoid bodies were transferred into gelatin-coated flasks, in MSC differentiation medium consisting of Knockout DMEM, 10% KSR, 1 mM L-Glutamine, 1x non-essential amino acids and 10 ng/ml bFGF (R&D System). Expanding mesodermal intermediates were fed every 3-4 days and when they reached confluency, they were passaged using 0.05% trypsin. After the first two passages, pluripotent stem cell-derived MSCs (hiPSC-1-MSCs, hiPSC-2-MSCs, hESC-MSCs) were expanded in non-coated flasks, in the same conditions as for BM-MSCs. Samples from both initial BM-MSC lines that were used for hiPSC derivation were thawed and expanded in parallel cultures in order to be used for comparative assessment of the proliferative and chondrogenic characteristics of the PSC-MSCs.

Cell proliferation assay

All MSC populations were serially passaged till senescence. For assessment of the population doublings and population doubling time, during each passaging, cells were counted before seeding in new flasks. Population doublings were measured according to the formula $PD=(lnN-lnN_0)/ln2$ where N_0=initial number of cells seeded in flask, N=terminal number of cells in flask at time of passaging. Population doubling time was estimated according to the formula $PDT=T/PD$, where T=time between two passages measured in days.

Surface antigen expression analysis

For flow cytometry analysis, hiPSC-MSCs (passage 4) were harvested, washed and incubated with specific MSC marker antibodies CD90-FITC, CD44-PE, CD105-FITC, CD73-PE, CD34-PE, CD45-FITC. A Cytomics FC500 was used by Beckman Coulter with CXP software for the Cytomics FC500 flow cytometry system version 2, 2. We used 400 μL from the total volume of 1 mL hiPSC-MSCs in order to count the total number of cells and their viability, by adding 10 μl of 7-AAD for viable cells, using flow cytometry. Sample analysis was completed typically within 10 minutes.

Comparative genomic hybridization analysis (array-CGH)

Qiagen Blood Mini-kit was used for genomic DNA extraction from both hiPSC- (hiPSC-1 and hiPSC-2) and all of the MSC-samples. After further processing of, as previously described (Tzetis et al., 2012), the DNA was subsequently hybridized to Agilent SurePrint G3 Human 4x180K CGH+SNP microarrays. The array contains 110,712 [comparative genomic hybridization (CGH) + 59,647 [single-nucleotide polymorphism (SNP)] 60-mer oligonucleotide probes with 25.3-kb overall median probe spacing (5-kb in ISCA regions). Data extraction from raw microarray image files was achieved by using Agilent Feature Extraction Image Analysis Software (v. 10.7.3). Agilent Cyto Genomics (v. 2.7) software was then used in order to visualize and analyze the data as previously described (Tzetis et al., 2012).

Osteogenic and adipogenic differentiation of hiPSC-MSCs

hiPSC-MSCs (passage 4) were harvested, reseeded at appropriate concentrations in plates containing MesenCult Osteogenic Stimulatory Kit (Stem Cell Technologies, Vancouver, BC, Canada) and StemPro Adipogenesis Differentiation Kit (Gibco, BRL), for osteogenesis and adipogenesis, respectively and cultured as monolayer, according to the manufacturer's instructions. Assessment of the differentiated cells was carried out with staining techniques. Alizarin Red and Alkaline Phosphatase was used to stain osteocytes and Oil Red for adipocytes.

Chondrogenic differentiation of MSC lines

Chondrogenesis assay was similarly applied to hiPSC-MSCs, hESC-MSCs and BM-MSCs (all cell populations at passage 4) in order to obtain comparative results. $2.5x10^5$ MSCs were seeded as droplets into the centre of tissue culture 24-well plates to achieve attachment of the cells in high density and maintained in standard chondrogenic medium, StemPro Chondrogenesis Differentiation Kit (Gibco, BRL) for 3 weeks. The derived chondrogenic micromasses were analyzed histologically and immunohistochemically.

Histological and immunohistochemical analysis

All MSC-derived cartilage micromasses were formalin-fixed, paraffin-embedded and sectioned. For histological analysis, micromasses were stained with hematoxylin and eosin (H&E). Additional histological

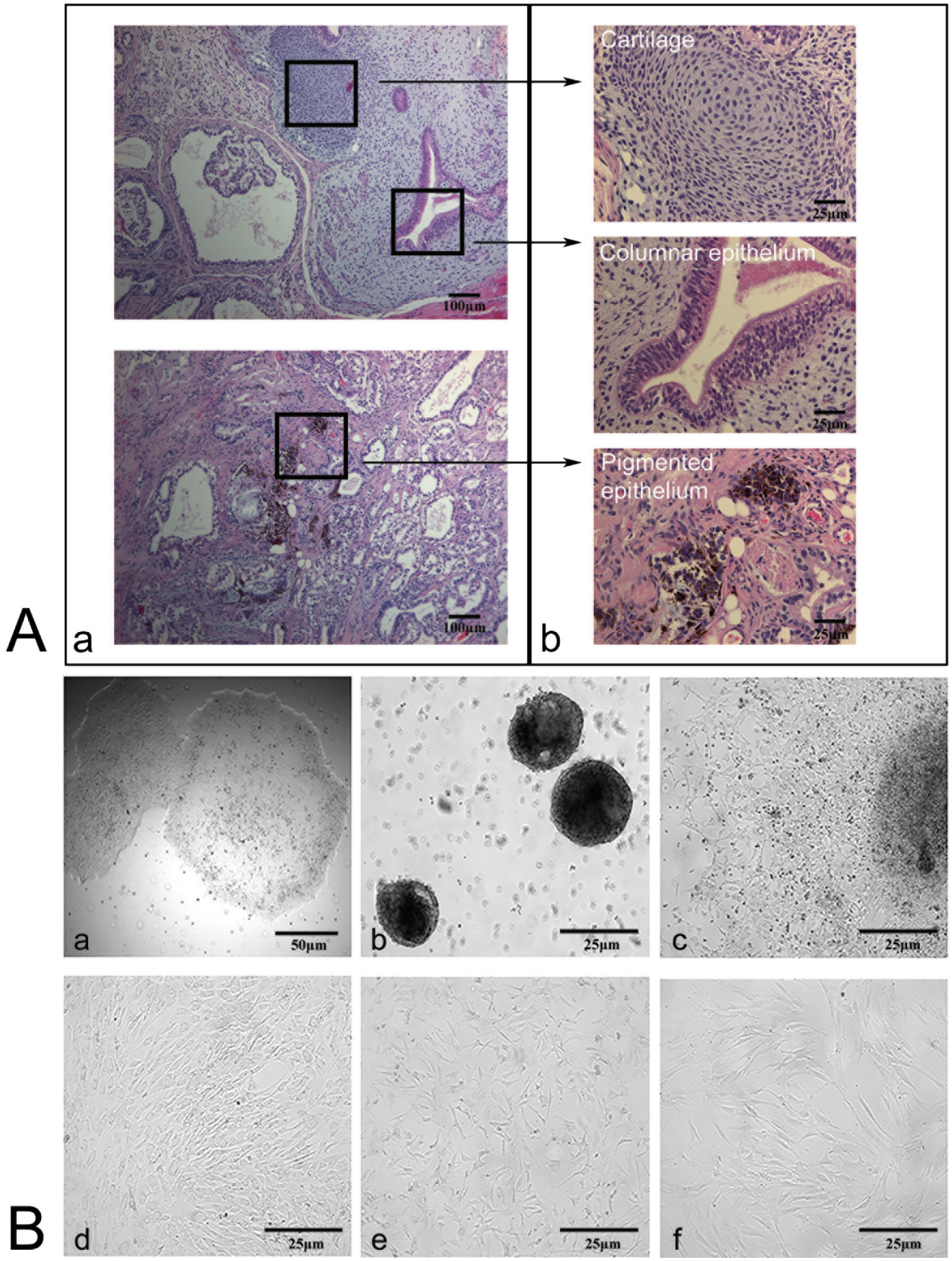

Fig. 1. A. *In vivo* teratoma formation, after injection of hiPSCs in NOD/SCID mice. a) Hematoxylin and eosin staining of the formed teratoma at magnification 10x, showing the presence of tissues that originate from all three germ layers (endoderm, ectoderm, mesoderm). b) Higher magnification (40x) depicts the formation of cartilage (mesoderm), columnar epithelium (endoderm) and pigmented epithelium (ectoderm) (Representative pictures of hiPSC-1 experiments). **B.** Generation of mesenchymal populations. a) Morphology of hiPSC colonies on Matrigel, before harvesting and induction of embryoid body formation. b) hiPSC-derived EBs after two days of culture into ultra-low attachment plate. c) hiPSC-derived EB three days after attachment on gelatin-coated surface. d, e, f) hiPSC-1-MSCs, hESC-MSCs and BM-MSCs at passage 3, respectively.

observations were performed after Alcian Blue staining. All immunostaining studies were performed on a Leica Bond-Max automated strainer platform (Leica Biosystems) employing a polymeric secondary detection system (Refine;Leica), using diaminobenzidine as a chromogen. The immunostaining protocol was tested and optimized. Immunohistochemistry for Sox9 was performed using a rabbit monoclonal antibody, clone EPR14335 (1/1000 dilution, Abcam, Cambridge, MA). A mouse monoclonal antibody, clone M2139, was used for the detection of COL2A1 (1/20 dilution, Santa Cruz Biotechnology, Dallas, TX). The cartilage of trephine bone marrow biopsies was used as a positive control.

Results

Generation and phenotype of MSCs

Prior to mesenchymal differentiation, hiPSC lines had been tested for pluripotency. The hiPSC lines expressed pluripotency genes and formed teratomas, after injections in NOD/SCID mice (Fig. 1A). All PSC lines proliferated on Matrigel until a sufficient number of cells was obtained for differentiation. PSC colonies (Fig. 1Ba) were then harvested and allowed to form EBs into ultra-low attachment plates. Aggregates formed compact spherical structures (Fig. 1Bb) in the first 2-3 days and grew in size by day 7, when they were harvested. When seeded on gelatin-coated surface, disaggregated EBs attached and within the first 2-3 days, proliferating cells with morphology resembling mesenchymal cells appeared in the periphery of each EB (Fig. 1Bc) and expanded rapidly, reaching confluency within 7 days of culture. The initial population was heterogeneous, but homogeneity increased with passaging. After 2-3 passages residual epithelioid cells were removed and the cell population consisted predominantly of cells with mesenchymal-like

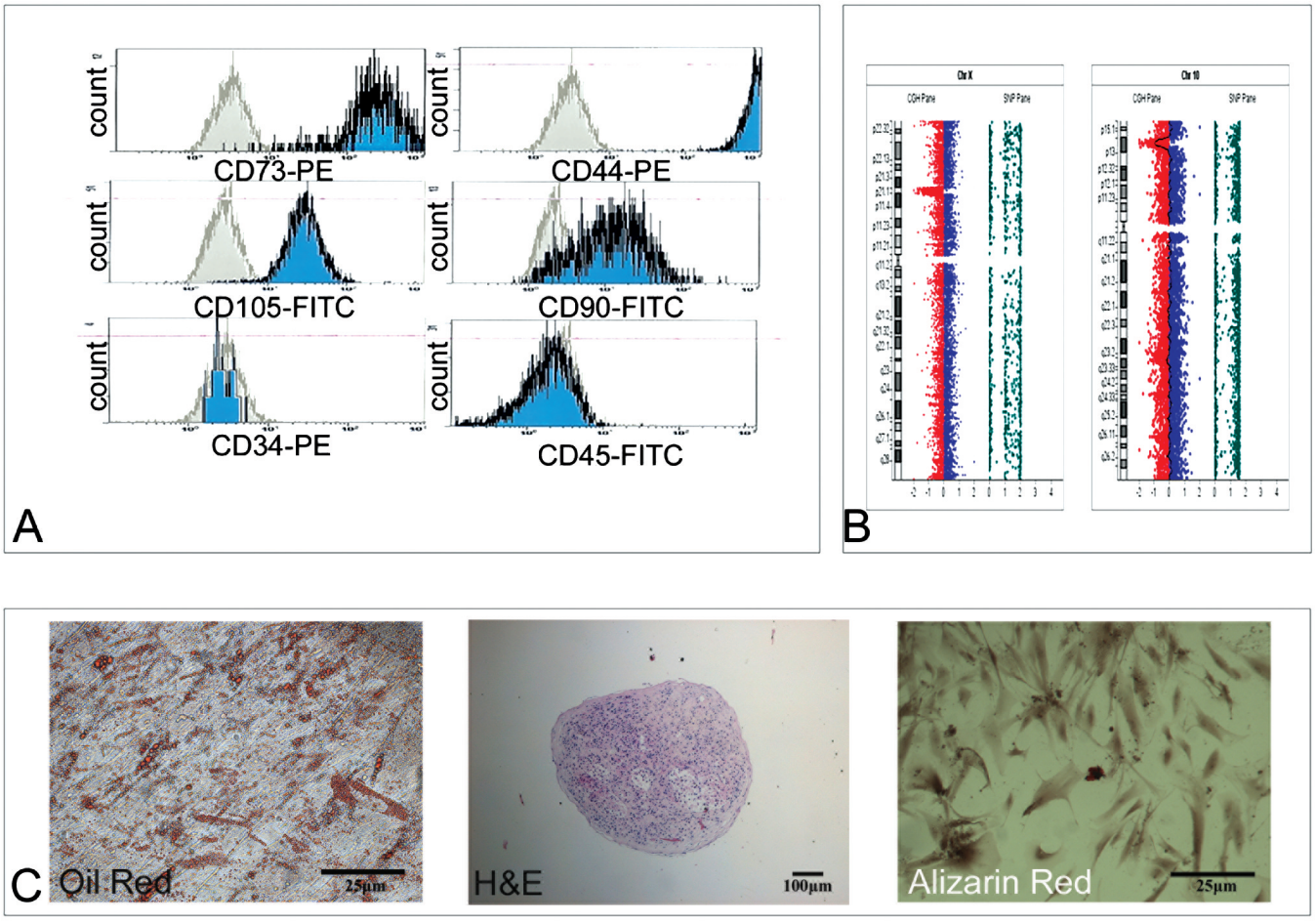

Fig. 2. Characteristics of hiPSC-MSCs. **A.** As revealed with flow cytometric analysis, MSCs express specific surface antigens CD90, CD44, CD105, CD73 and lack the expression of CD34 and CD45. **B.** Detection of deletions of approximately 3 Mb, in chromosomes X (DELXp21.3-p21.1) and 10 (DEL10p14), in hiPSC-1-MSCs and hiPSC-2-MSCs, respectively. **C.** Morphological identification of MSC-derived mesodermal tissues was achieved with Oil Red stain in adipogenic cultures, Alizarid Red in osteogenic cultures (arrows indicate extracellular calcium deposition) and with hematoxylin and eosin in chondrogenic micromasses (Representative pictures).

morphology. The time required for generation of an MSC population from undifferentiated hiPSC-1 and hiPSC-2 cell lines was approximately 3 weeks and was equivalent to that of Hues9 differentiation. Derivation of MSC populations from BM was achieved after 2 passages in a time interval of 3 weeks. hiPSC-MSCs similarly to hESC-MSCs, had the typical spindle-shaped morphology of BM-MSCs (Fig. 1Bd,e,f), while both displayed a smaller size than the latter. hiPSC-MSCs and hESC-MSCs expressed all specific MSC markers, CD73, CD105, CD90, CD44 and lacked expression of the hematopoietic markers CD34 and CD45 (Fig. 2A). Furthermore, all the PSC-MSC populations downregulated the expression of pluripotency genes *OCT3/4* and *NANOG* by passage 4, at levels similar to the BM-MSCs (Fig. 3).

Proliferation of MSCs

All MSC populations were cultured until senescence in order to compare their proliferative properties. Proliferation capacity of hiPSC-MSCs and hESC-MSCs decreased during continuous passaging, in accordance with BM-MSCs. hiPSC-1- and hiPSC-2-MSC proliferation ceased completely after 25 and 20 passages, respectively. Related results obtained from hESC-MSCs and the 2 BM-MSC-lines were 19, 13 and 14 passages, respectively. Due to the much smaller size of PSC-MSCs, each confluent 25 cm^2 flask during at least the first 8-10 passages yielded an average of $1.5x10^6$ cells ($6x10^4/cm^2$), whereas for BM-MSCs each flask yielded $7x10^5$ cells ($2{,}8x10^4/cm^2$) or below. Comparative results of the number of population doublings, average population doubling time, maximum total cell yields and fold expansion of all MSC populations are shown in Table 1. Proliferative potential of PSC-MSCs according to these parameters was found to be higher compared to BM-MSCs. The elevated growth rates of hiPSC- and hESC-MSC populations are depicted in Fig. 4.

Genetic stability of derived MSCs

As revealed with array-CGH, initial BM-MSCs had a normal chromosomal pattern and only exhibited polymorphic variants (Copy number Polymorphisms-CNPs) in their genome. hiPSC-1 and hiPSC-2 lines had normal karyotypes, but at the molecular level they had acquired after 10 passages one deletion of approximately 3 Mb, in chrX: 29182625- 32011209 (DEL Xp21.3-p21.1) and chr10: 6998908- 10013116 (DEL10p14), respectively (reference genome hg19) (Fig. 2B). These deletions had occurred during continuous passaging, as has been extensively observed in PSC cultures and the phenomenon is related to culture adaptation. The affected regions did not contain genes involved in cell growth and proliferation. hiPSC-MSCs maintained the same chromosomal pattern as their hiPSC ancestors before differentiation. The Hues9 line is already well characterized genetically. The derived hESC-MSCs exhibited the same chromosomal pattern as the maternal hESCs.

In vivo tumor generation assay

After injection of PSC-MSCs into NOD/SCID mice, no tumor formation was observed in a maximum time interval of 10 weeks.

In vitro adipogenic and osteogenic differentiation capacity of hiPSC-MSCs

In order to prove their osteogenic and adipogenic capacity, the derived hiPSC-MSC lines were cultured in standard osteogenic and adipogenic conditions. Osteogenesis was evident from the first two weeks by typical calcium deposition sites on the cell layer. Alizarid Red Stain after 35 days of culture confirmed the presence of osteogenic activity (Fig. 2C). Additionally, Alkaline Phosphatase activity was detected and further

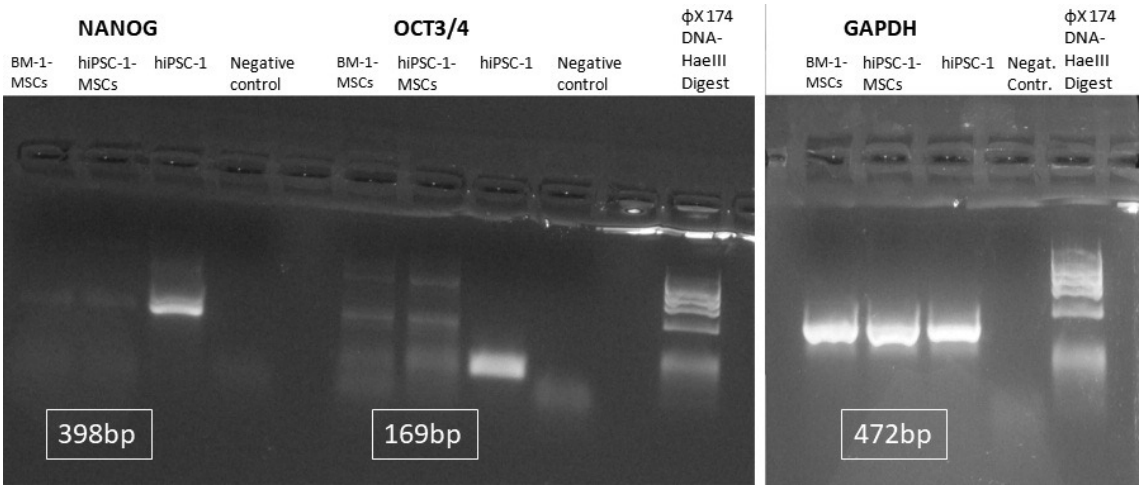

Fig. 3. Downregulation of pluripotency markers in PSC-MSCs. Representative results of RT-PCR from passage 4 hiPSC-1-MSCs, showing the downregulation of NANOG and OCT3/4 expression at levels similar to the initial BM-1-MSCs. Housekeeping GAPDH gene expression was used as internal control.

supported differentiation (data not shown). Culture of MSCs in adipogenic medium also resulted in adipocytic phenotype. Oil Red Stain revealed accumulation of lipid droplets in the cells (Fig. 2C).

Comparison of chondrogenic differentiation among MSC populations

In order to focus on chondrogenic differentiation capacity and assess the quality of cartilage, derived from hiPSC-MSCs and hESC-MSCs compared to BM-MSCs, chondrogenic micromasses were analyzed in all MSC samples, after culture under the same chondrogenic conditions for 3 weeks. All MSCs under these conditions formed compact spherical structures. Histological and immunohistochemical findings are shown in Fig. 5. Based on the results, BM-MSC-derived cartilage displayed a highly acidic extracellular matrix, as indicated by the deep bluish colour in H&E, thus rich in the proteoglycans that define mature hyaline cartilage. Furthermore, the tissue was abundant in lacunae that contained mature spherical chondrocyte-like cells. On the other hand, PSC-derived MSCs failed to form typical hyaline cartilage, but showed some degree of chondrogenesis, with the derived tissue having a pinkish, rather than deep blue colour in the extracellular area in H&E staining, in contrast to BM-MSC derived cartilage. High cellularity, with an abundance of small-sized, immature cells and a general lack of the typical lacunae organization were observed in PSC-MSC tissues. Additionally, there was a high proportion of cells having a spindle, mesenchymal morphology. The overall histological picture resembles pink rather than hyaline cartilage. and the findings suggest a possible incomplete chondrogenesis process (Fig. 5). Further histological observation after Alcian Blue staining verified those findings, indicating much less blue-stained GAG content in PSC-MSC-derived cartilage (Fig. 6). Immunohistochemistry for Sox9 protein revealed that in BM-MSC-derived micromasses as high as 80% of cells showed remarkable expression, while in contrast, in hiPSC-MSC derived micromasses, approximately 1% of cells expressed the marker (Fig. 5). In hiPSC-MSC derived micromasses staining was poor even in cells that expressed the marker, indicating low levels of expression. In hESC-derived micromasses there was some expression of Sox9 of about 40%, but this was localized in a small region of the tissue that lacked hyaline cartilage morphology, unlike BM-MSC derived ones (Fig.5). As indicated by immunohistochemistry with anti-COL2A1 antibody, COL2A1 was remarkably produced in BM-derived micromasses and could be observed in approximately 70% of the matrix surrounding the chondrocytes throughout the micromass. Production of COL2A1 appeared to be co-localized with Sox9 expression. In hiPSC- and hESC-derived micromasses, there was no COL2A1 production observed (0% of the tissue). In hESC-derived micromasses, Sox9 expression did not correlate with COL2A1 production (Fig. 5).

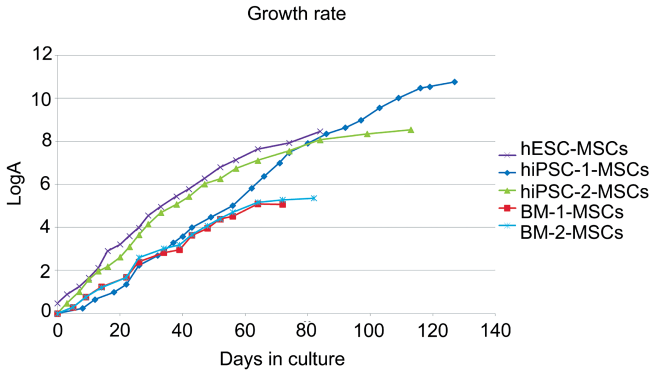

Fig. 4. Growth rate of MSC populations. Each graph shows the logarithmic fold expansion (LogA) during culture of (hiPSC)-, (hESC)- and BM-derived MSCs, where A represents the cumulative number of MSCs produced after each passage divided by the initial number of cells at the beginning of the culture. The dots on the graph represent the additional passages of the MSC populations.

Discussion

The properties of MSCs have been extensively investigated for many years and can possibly be beneficial for the treatment of inflammatory and

Table 1. Comparative depiction of the proliferative characteristics of hiPSC-, hESC- and BM-MSCs.

	Number of passages	Population doublings	Population doubling time (days)	Total number of cells produced	Fold expansion
hiPSC-1-MSCs	25	35.7	3.3	$1.41x10^{17}$	$5.88x10^{10}$
hiPSC-2-MSCs	20	28.3	3.3	$9x10^{14}$	$3.49x10^{8}$
hESC-MSCs	19	28.1	3.08	$6x10^{14}$	$2.88x10^{8}$
BM-1-MSCs	13	16.9	3.9	$8.5x10^{10}$	$1.18x10^{5}$
BM-2-MSCs	14	17.8	3.9	$1.7x10^{11}$	$2.3x10^{5}$

hiPSCs: human induced pluripotent stem cells, hESCs: human embryonic stem cells, BM: bone marrow MSCs: mesenchymal stromal cells, hiPSC-1-MSCs; hiPSC-2-MSCs: MSC lines derived from hiPSCs, hESC-MSCs: MSC line derived from hESCs, BM-1-MSCs; BM-2-MSCs: MSC lines derived from BM.

degenerative diseases. The perspective of utilizing hiPSCs for the production of MSCs has already been described (Sabapathy and Kumar, 2016). PSCs represent an attractive source of MSCs, as they can be indefinitely expanded and stored in large quantities in liquid nitrogen, thus being constantly available for differentiation. In this study, mesenchymal differentiation of PSCs was achieved with high efficiencies in a time interval of 3 weeks. We used the protocol of EB formation, in which, initial differentiation into all three germ layers takes place. The derived cells expressed MSC-specific surface antigens and they had a uniform appearance with typical spindle-shaped MSC morphology, while their size was smaller and they had a more juvenile appearance than adult MSCs. Differentiation did not cause any chromosomal aberrations in the derived MSCs and all lines maintained the chromosomal pattern of their parental PSCs. The iPSC-derived lines had maintained a few CNPs that are not related to aberrant cell growth. PSC-MSCs were examined for their proliferative characteristics in comparison with BM-MSC, which are currently used in preclinical and clinical studies (Sabapathy and Kumar, 2016). Their proliferative capacity appeared much higher compared to that of BM-MSCs, as they could be expanded for a higher number of passages and, most

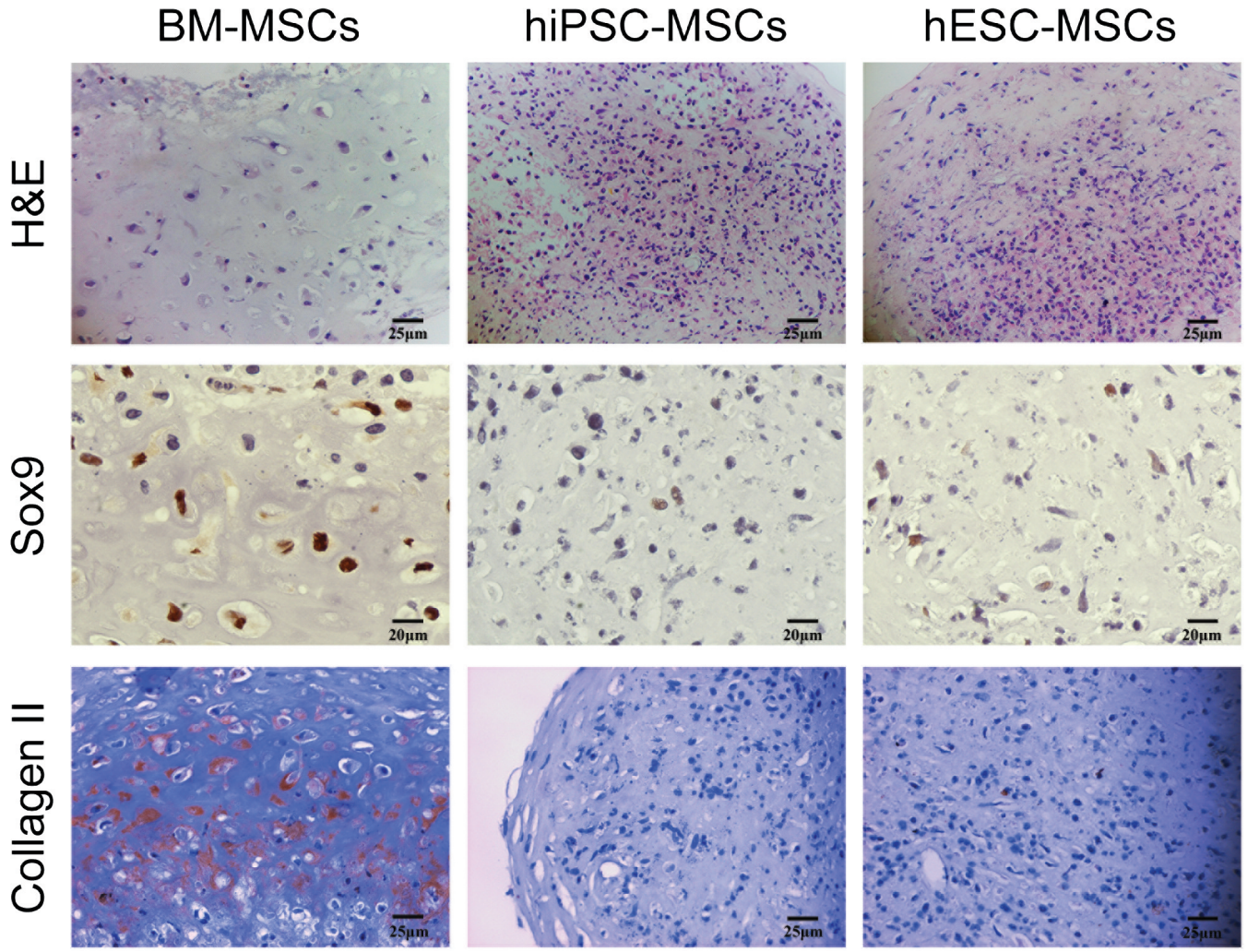

Fig. 5. Histological and immunohistochemical analysis of BM and PSC-derived cartilage micromasses. BM-derived micromasses display typical histological hyaline cartilage features, with an abundance of bluish acidic extracellular matrix, low cellularity and the presence of lacunae containing mature chondrocytes. Sox9 protein was detected in a high proportion of cells and COL2A1 was produced in the area surrounding the chondrocytes throughout the micromass. hiPSC-derived cartilage micromasses display high cellularity, a high proportion of spindle shaped and immature cells, lack of lacunae and pinkish extracellular matrix in hematoxylin and eosin staining. Expression of Sox9 was very weak and COL2A1 production was absent. hESC-derived micromasses display similar morphological features to hiPSC-derived cartilage, much lower Sox9 expression than BM-MSCs and absence of COL2A1 production. (Pictures of a representative experiment).

importantly, yielded a much higher amount of cells. hiPSC-MSCs and hESC-MSCs reached higher numbers of population doublings than BM-MSCs. Fold expansion appeared to be up to $5x10^5$ times greater for hiPSC-MSCs and $2.5x10^3$ for hESC-MSCs in comparison to BM-MSCs. Nevertheless, PSC- derived MSCs appeared to enter in senescence after prolonged passaging, like normal adult MSCs. The higher proliferative capacity of PSC- derived MSCs is in line with other previously reported results. Several researchers have reported that PSC-derived MSCs were able to reach 2 times the number of population doublings observed in BM-MSCs and had a fold expansion that was $3x10^4$ times higher (Wei et al., 2012; Kimbrel et al., 2014). Other groups also showed that hiPSC-derived MSCs had a more rapid growth than BM-MSCs, with significantly shorter doubling time (Zhao et al., 2015; Sheyn et al., 2016). Interestingly, Lian et al. managed to expand a hiPSC-MSC line for up to 40 passages (120 population doublings), without observing any chromosomal alterations and showed that passage 36 hiPSC-MSCs exhibited 10 times the telomerase activity of passage 6 BM-MSCs (Lian et al., 2010). Our study further supports that PSC lines can generally produce MSCs with more robust proliferation characteristics than BM-MSCs, producing large amounts of cells with the potential to be used for cellular therapy.

Regarding multi-lineage differentiation capacity of hiPSC-MSCs, our study showed that they were capable of generating osteoblasts and adipocytes *in vitro*. A more thorough investigation was attempted on the chondrogenic capacity of PSC-MSCs, in order to assess the possibility of generating articular cartilage with equal or better quality to that of BM-MSCs, for potential clinical applications for the treatment of degenerative joint diseases. To compare the differentiation potential of PSC-MSCs to that of BM-MSCs, we considered passage 4 as an appropriate time point at which the mesenchymal differentiation of PSC-MSCs had already been completed and the derived MSCs were phenotypically close to BM-MSCs. Our criteria for choosing the appropriate passage of PSC-MSCs to use for further differentiation was the MSC-like morphology and the characteristic BM-MSC immunophenotype of the derived cells. Those features already existed at passage 4, when chondrogenic differentiation was examined, as they expressed the MSC-specific markers in >95% and had similar morphology to BM-MSCs. The morphology and immunophenotype of a later passage (passage 7) PSC-MSCs did not show any difference from passage 4 PSC-MSCs. Furthermore, all the derived populations at passage 4 had already downregulated expression of *OCT3/4* and *NANOG* pluripotency genes, at levels similar to BM-MSCs. Thus, at this point we considered the PSC-MSC population phenotypically similar to BM-MSCs. After culture in a commercial chondrogenic medium typically used for BM-MSCs, we evaluated the morphology of the derived chondrogenic tissues and the expression of proteins that play critical roles in cartilage, in comparison with BM-MSC-derived ones. Histological analysis after H&E staining showed that hiPSC-MSC and hESC-MSC chondrogenic micromasses did not have typical hyaline cartilage morphology, in contrast to BM-derived cartilage, and had a lower content in cartilage proteoglycans and more spindle-shaped cells. The expression of Sox9, a transcription factor that plays a crucial role in chondrogenesis and characterizes functional chondrocytes in articular cartilage, was much lower in hESC-MSC- and absent in hiPSC-MSC-derived cartilage, whereas BM-MSC-derived cartilage was abundant in cells expressing the marker. Immunohistochemistry for COL2A1, the major protein that constitutes the extracellular matrix of hyaline cartilage, showed abundant production in BM-MSC derived micromasses, but, in contrast, no protein was detected in PSC-MSC derived micromasses. The differences in the morphology of the cartilage and in the expression of major cartilage-specific proteins, among

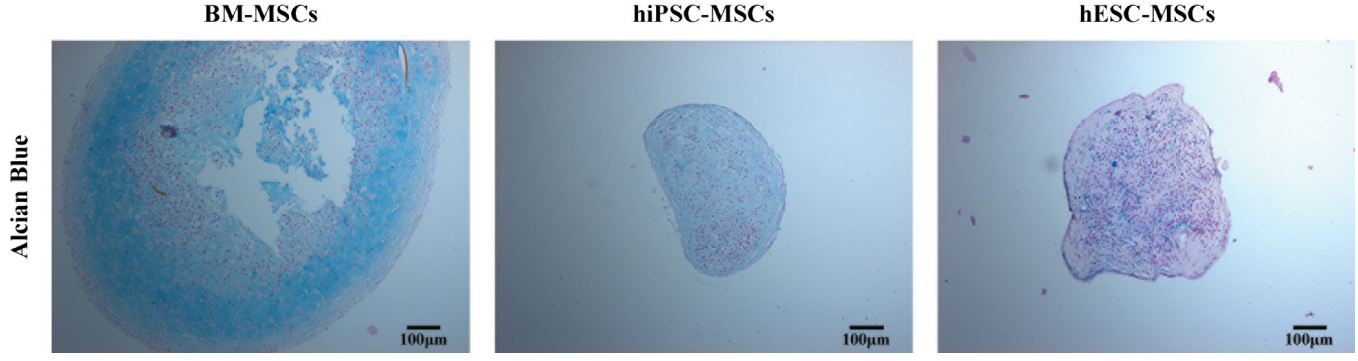

Fig. 6. Alcian Blue staining of the MSC-derived chondrogenic micromasses. After 3 weeks in chondrogenic cultures, BM-MSC-, hiPSC-MSC- and hESC-MSC-derived tissues were stained with Alcian Blue. The staining revealed that PSC-MSC tissues had much less intense blue stained extracellular matrix than BM-MSC derived cartilage, indicating much less content in acidic proteoglycans. Pictures are representative from one experiment of hiPSC-1-MSCs.

the PSC- and BM- derived MSCs, give a strong indication of inefficient *in vitro* chondrogenesis process of PSC-MSCs. In this work, we aimed at applying exactly the same chondrogenic conditions for BM-MSCs and PSC-MSCs, in order to assess whether the standard conditions used for BM-MSC differentiation are adequate for obtaining similar results with PSC-MSCs. During our experiments, we additionally maintained some of the differentiating micromasses for 25 instead of 21 days which was the typical time required in the protocol, but the histological H&E picture was similar, suggesting pink rather than typical hyaline cartilage formation. Our results indicate that under the same conditions, PSC-MSCs which are phenotypically similar to BM-MSCs exhibit inefficient chondrogenesis.

Several studies, based on proteoglycan staining (Lian et al., 2007; Wei et al., 2012; Kimbrel et al., 2014) or upregulation of mRNA expression of chondrogenic markers (Lian et al., 2007), report a cartilage formation capability of PSC-MSCs. Kang et al. found that MSCs derived from two hiPSC lines were capable of generating osteocytes and chondrocytes similar to BM-MSCs, although their ability to generate adipocytes was impaired (Kang et al., 2015). Other publications report robust chondrogenic differentiation of PSC-MSCs (Moslem et al., 2015; Zhao et al., 2015; Nam et al., 2017). Our finding is in line with the results of two other studies that compared the properties of BM- and hiPSC-derived MSCs and found that the latter were less efficient for *in vitro* chondrogenic differentiation, according to the standard protocols used for BM-MSCs (Diederichs and Tuan, 2014; Xu et al., 2019). Our study observed chondrogenesis defects not only in hiPSC-MSCs, but also in the hESC-MSC line, which is derived from "true" embryonic stem cells.

It has been hypothesized that PSC-derived MSCs may possibly serve as substitutes of adult tissue-derived MSCs for tissue regeneration. Currently, BM-MSCs are being used in numerous preclinical and clinical studies worldwide, including research on osteoarthritis (OA) treatment. Cellular therapy of OA has for many years mainly been based on Autologous Chondrocyte Implantation (ACI), which involves several limitations, such as donor-site morbidity, dedifferentiation of chondrocytes during *in vitro* expansion and poor integration (Burke et al., 2016). Clinical studies that use MSC injection techniques in patients with affected joints demonstrate beneficial results. Centeno et al. have reported on 339 patients, 69% of which needed total joint replacement. After local injection of autologous BM-MSCs, only 6.9% still required surgery, while 60% of the patients reported >50% pain relief (Centeno et al., 2011). Vega et al. reported that 12 months after injection with allogenic BM-MSCs, the 15 patients that were MSC-treated had both pain and functional improvement versus the control group (Vega et al., 2015). Autologous BM-MSC injection in another study showed pain and functional improvement in all 6 patients and increase in cartilage thickness in 3 patients (Emadedin et al., 2012). Therefore, the utilization of BM-MSCs for cartilage regeneration seems to be feasible, but still under investigation. On the other hand, several studies have focused during the last years on the derivation of chondrocytes directly from PSCs using various protocols. These attempts have promising results, showing engraftment and survival of the derived cartilaginous tissue in cartilage defects of osteoarthritis animal models (Nejadnik et al., 2015; Yamashita et al., 2015; Zhu et al., 2016; Kawata et al., 2019).

Although PSC-derived MSCs exhibit great similarities with BM-MSCs, the finding that *in vitro* cartilage formation appears to be inefficient using the standard protocols that are commonly used for BM-MSCs, needs to be further investigated. It is known that there are differences in multilineage differentiation potential between MSCs derived from different adult tissues (Giai Via et al., 2012), with BM-MSCs displaying superior *in vitro* chondrogenesis than adipose and muscle derived MSCs (Giai Via et al., 2012; Sakaguchi et al., 2005). In the case of hiPSC-derived MSCs, there are also some indications that their multilineage differentiation properties depend on the initial adult somatic cells, from which they are derived (Hynes et al., 2014). One study has reported different multilineage differentiation properties among hiPSC-MSCs derived from different hiPSC clones of the same person (Nasu et al., 2013).

The inferior results in chondrogenesis of PSC-MSCs in the current study do not necessarily indicate an endogenous defect of PSCs to differentiate. The protocols of mesenchymal differentiation might play an important role in the properties of derived cells (Diederichs and Tuan, 2014; Xu et al., 2019). Recent work, by our team, found that PSC-MSCs had inferior anti-inflammatory effect than bone marrow and umbilical cord blood MSCs in a mouse model of inflammatory bowel disease, in terms of survival prolongation, macroscopic and histopathological picture improvement of colon (Kagia et al., 2019). Optimization of the protocols would be crucial in order to obtain MSCs with the same abilities as BM-MSCs. Xu et al., after gene expression analysis in hiPSC-MSCs and BM-MSCs were led to the conclusion that hiPSC-MSCs were closer to vascular progenitor cells, as they exhibited $KDR^{high}MSX2^{high}PDGFRa^{low}$ phenotype, containing low levels of MSC-like cells (Xu et al., 2019). PSC-MSCs as a distinct population from BM-MSCs may have different *in vitro* requirements for multilineage differentiation than BM-MSCs. Attempts have already been made to better understand these requirements and enhance differentiation potential (Guzzo et al., 2013). Future studies should focus on the mesenchymal differentiation protocols of PSCs, epigenetic differences between BM-MSCs and those derived from PSCs. Finally, *in vivo* experiments are the most appropriate to assess the function of PSC-MSCs in comparison with BM-MSCs in osteoarthritic animal models and will elucidate the therapeutic potential of these cells.

Acknowledgements. This work was partially funded by a research program EPAnEK 2014-2020, Operational Programme Competitiveness-entrepreneurship-innovation, in which our team is involved.

References

Awaya T., Kato T., Mizuno Y., Chang H., Niwa A., Umeda K., Nakahata T. and Heike T. (2012). Selective development of myogenic mesenchymal cells from human embryonic and induced pluripotent stem cells. PLoS One 7, e51638

Burke J., Hunter M., Kolhe R., Isales C., Hamrick M. and Fulzele S. (2016). Therapeutic potential of mesenchymal stem cell based therapy for osteoarthritis. Clin. Transl. Med. 5, 27.

Centeno C.J., Schultz J.R., Cheever M., Freeman M., Faulkner S., Robinson B. and Hanson R. (2011). Safety and complications reporting update on the re-implantation of culture-expanded mesenchymal stem cells using autologous platelet lysate technique. Curr. Stem Cell Res. Ther. 6, 368-378.

Chen Y.S., Pelekanos R.A., Ellis R.L., Horne R., Wolvetang E.J. and Fisk N.M. (2012). Small molecule mesengenic induction of human induced pluripotent stem cells to generate mesenchymal stem/stromal cells. Stem Cells Transl. Med. 1, 83-95.

Diederichs S. and Tuan R.S. (2014). Functional comparison of human-Induced pluripotent stem cell-derived mesenchymal cells and bone marrow-derived mesenchymal stromal cells from the same donor. Stem Cells Dev. 23, 1594-1610.

Dominici M., Le Blanc K., Mueller I., Slaper-Cortenbach I., Marini F., Krause D., Deans R., Keating A., Prockop D. and Horwitz E. (2006). Minimal criteria for defining multipotent mesenchymal stromal cells. The International Society for Cellular Therapy position statement. Cytotherapy 8, 315-317.

Emadedin M., Aghdami N., Taghiyar L., Fazeli R., Moghadasali R., Jahangir S., Farjad R. and Baghaban Eslaminejad M. (2012). Intra-articular injection of autologous mesenchymal stem cells in six patients with knee osteoarthritis. Arch. Iran. Med. 15, 422-428.

Giai Via A., Frizziero A. and Oliva F. (2012). Biological properties of mesenchymal stem cells from different sources. Muscles Ligaments Tendons J. 2, 154-162.

Giuliani M., Oudrhiri N., Noman Z.M., Vernochet A., Chouaib S., Azzarone B., Durrbach A. and Bennaceur-Griscelli A. (2011). Human mesenchymal stem cells derived from induced pluripotent stem cells down-regulate NK-cell cytolytic machinery. Blood 118, 3254-3262.

Guzzo R.M., Gibson J., Xu R.-H., Lee F.Y. and Drissi H. (2013). Efficient differentiation of human iPSC-derived mesenchymal stem cells to chondroprogenitor cells. J. Cell. Biochem. 114, 480-490.

Hass R., Kasper C., Böhm S. and Jacobs R. (2011). Different populations and sources of human mesenchymal stem cells (MSC): A comparison of adult and neonatal tissue-derived MSC. Cell Commun. Signal. 9, 12.

Hynes K., Menicanin D., Mrozik K., Gronthos S. and Bartold P.M. (2014). Generation of functional mesenchymal stem cells from different induced pluripotent stem cell lines. Stem Cells Dev. 23, 1084-1096.

Kagia A., Tzetis M., Kanavakis E., Perrea D., Sfougataki I., Mertzanian A., Varela I., Dimopoulou A., Karagiannidou A. and Goussetis E. (2019). Therapeutic effects of mesenchymal stem cells derived from bone marrow, umbilical cord blood, and pluripotent stem cells in a mouse model of chemically induced inflammatory bowel disease. Inflammation 42, 1730-1740.

Kang R., Zhou Y., Tan S., Zhou G., Aagaard L., Xie L., Bünger C., Bolund L. and Luo Y. (2015). Mesenchymal stem cells derived from human induced pluripotent stem cells retain adequate osteogenicity and chondrogenicity but less adipogenicity. Stem Cell Res. Ther. 6, 144.

Karagiannidou A., Varela I., Giannikou K., Tzetis M., Spyropoulos A., Paterakis G., Petrakou E., Theodosaki M., Goussetis E. and Kanavakis E. (2014). Mesenchymal derivatives of genetically unstable human embryonic stem cells are maintained unstable but undergo senescence in culture as do bone marrow-derived mesenchymal stem cells. Cell. Reprogramming 16, 1-8.

Kawata M., Mori D., Kanke K., Hojo H., Ohba S., Chung U., Yano F., Masaki H., Otsu M., Nakauchi H., Tanaka S. and Saito T. (2019). Simple and robust differentiation of human pluripotent stem cells toward chondrocytes by two small-molecule compounds. Stem Cell Rep. 13, 530-544.

Kimbrel E.A., Kouris N.A., Yavanian G.J., Chu J., Qin Y., Chan A., Singh R.P., McCurdy D., Gordon L., Levinson R.D. and Lanza R. (2014). Mesenchymal stem cell population derived from human pluripotent stem cells displays potent immunomodulatory and therapeutic properties. Stem Cells Dev. 23, 1611-1624.

Lian Q., Lye E., Suan Yeo K., Khia Way Tan E., Salto-Tellez M., Liu T.M., Palanisamy N., El Oakley R.M., Lee E.H., Lim B. and Lim S.-K. (2007). Derivation of clinically compliant MSCs from CD105+, CD24-differentiated human ESCs. Stem Cells 25, 425-436.

Lian Q., Zhang Y., Zhang J., Zhang H.K., Wu X., Zhang Y., Lam F.F.-Y., Kang S., Xia J.C., Lai W.-H., Au K.-W., Chow Y.Y., Siu C.-W., Lee C.-N. and Tse H.-F. (2010). Functional mesenchymal stem cells derived from human induced pluripotent stem cells attenuate limb ischemia in mice. Circulation 121, 1113-1123.

Liu Y., Goldberg A.J., Dennis J.E., Gronowicz G.A. and Kuhn L.T. (2012). One-step derivation of mesenchymal stem cell (MSC)-like cells from human pluripotent stem cells on a fibrillar collagen coating. PloS One 7, e33225.

Moslem M., Eberle I., Weber I., Henschler R. and Cantz T. (2015). Mesenchymal stem/stromal cells derived from induced pluripotent stem sells support CD34(pos) hematopoietic stem cell propagation and suppress inflammatory reaction. Stem Cells Int. 2015, 843058.

Murphy M.B., Moncivais K. and Caplan A.I. (2013). Mesenchymal stem cells: environmentally responsive therapeutics for regenerative medicine. Exp. Mol. Med. 45, e54.

Nam Y., Rim Y.A., Jung S.M. and Ju J.H. (2017). Cord blood cell-derived iPSCs as a new candidate for chondrogenic differentiation and cartilage regeneration. Stem Cell Res. Ther. 8.

Nasu A., Ikeya M., Yamamoto T., Watanabe A., Jin Y., Matsumoto Y., Hayakawa K., Amano N., Sato S., Osafune K., Aoyama T., Nakamura T., Kato T. and Toguchida J. (2013). Genetically matched human iPS cells reveal that propensity for cartilage and bone differentiation differs with clones, not cell type of origin. PLoS One 8, e53771.

Nejadnik H., Diecke S., Lenkov O.D., Chapelin F., Donig J., Tong X., Derugin N., Chan R.C.F., Gaur A., Yang F., Wu J.C. and Daldrup-Link H.E. (2015). Improved approach for chondrogenic differentiation of human induced pluripotent stem cells. Stem Cell Rev. 11, 242-253.

Nejadnik H., Hui J.H., Feng Choong E.P., Tai B.-C. and Lee E.H. (2010). Autologous bone marrow-derived mesenchymal stem cells versus autologous chondrocyte implantation: an observational cohort study. Am. J. Sports Med. 38, 1110-1116.

Sabapathy V. and Kumar S. (2016). hiPSC-derived iMSCs: NextGen MSCs as an advanced therapeutically active cell resource for regenerative medicine. J. Cell. Mol. Med. 20, 1571-1588.

Sakaguchi Y., Sekiya I., Yagishita K. and Muneta T. (2005). Comparison of human stem cells derived from various mesenchymal tissues: Superiority of synovium as a cell source. Arthritis Rheum. 52, 2521-2529.

Sharma R.R., Pollock K., Hubel A. and McKenna D. (2014). Mesenchymal stem or stromal cells: a review of clinical applications and manufacturing practices. Transfusion 54, 1418-1437.

Sheyn D., Ben-David S., Shapiro G., De Mel S., Bez M., Ornelas L., Sahabian A., Sareen D., Da X., Pelled G., Tawackoli W., Liu Z., Gazit D. and Gazit Z. (2016). Human induced pluripotent stem cells differentiate into functional mesenchymal stem cells and repair bone defects. Stem Cells Transl. Med. 5, 1447-1460.

Tang M., Chen W., Liu J., Weir M.D., Cheng L. and Xu H.H.K. (2014). Human induced pluripotent stem cell-derived mesenchymal stem cell seeding on calcium phosphate scaffold for bone regeneration. Tissue Eng. Part A 20, 1295-1305.

Toh W.S. (2016). Pluripotent stem cells: Differentiation potential and therapeutic efficacy for cartilage repair. In: Pluripotent stem cells - from the bench to the clinic. Chapter: 17. Tomizawa M. (ed). InTechOpen. pp 363-384.

Tzetis M., Kitsiou-Tzeli S., Frysira H., Xaidara A. and Kanavakis E. (2012). The clinical utility of molecular karyotyping using high-resolution array-comparative genomic hybridization. Expert Rev. Mol. Diagn. 12, 449-457.

Varela I., Karagiannidou A., Oikonomakis V., Tzetis M., Tzanoudaki M., Siapati E.-K., Vassilopoulos G., Graphakos S., Kanavakis E. and Goussetis E. (2014). Generation of human β-thalassemia induced pluripotent cell lines by reprogramming of bone marrow-derived mesenchymal stromal cells using modified mRNA. Cell. Reprogramming 16, 447-455.

Vega A., Martín-Ferrero M.A., Del Canto F., Alberca M., García V., Munar A., Orozco L., Soler R., Fuertes J.J., Huguet M., Sánchez A. and García-Sancho J. (2015). Treatment of knee osteoarthritis with allogeneic bone marrow mesenchymal stem cells: A randomized controlled trial. Transplantation 99, 1681-1690.

Villa-Diaz L.G., Brown S.E., Liu Y., Ross A., Lahann J., Parent J.M. and Krebsbach P.H. (2012). Derivation of functional mesenchymal stem cells from human induced pluripotent stem cells cultured on synthetic polymer substrates. Stem Cells 30, 1174-1181.

Wang S., Qu X. and Zhao R.C. (2012). Clinical applications of mesenchymal stem cells. J. Hematol. Oncol. J. Hematol. Oncol. 5, 19.

Warren L., Manos P.D., Ahfeldt T., Loh Y.-H., Li H., Lau F., Ebina W., Mandal P.K., Smith Z.D., Meissner A., Daley G.Q., Brack A.S., Collins J.J., Cowan C., Schlaeger T.M. and Rossi D.J. (2010). Highly efficient reprogramming to pluripotency and directed differentiation of human cells with synthetic modified mRNA. Cell Stem Cell 7, 618-630.

Wei H., Tan G., Manasi Qiu, S., Kong G., Yong P., Koh C., Ooi T.H., Lim S.Y., Wong P., Gan S.U. and Shim W. (2012). One-step derivation of cardiomyocytes and mesenchymal stem cells from human pluripotent stem cells. Stem Cell Res. 9, 87-100.

Xu M., Shaw G., Murphy M. and Barry F. (2019). Induced pluripotent stem cell derived mesenchymal stromal cells are functionally and genetically different from bone marrow derived mesenchymal stromal cells. Stem Cells 37, 754-765.

Yamashita A., Morioka M., Yahara Y., Okada M., Kobayashi T., Kuriyama S., Matsuda S. and Tsumaki N. (2015). Generation of scaffoldless hyaline cartilaginous tissue from human iPSCs. Stem Cell Rep. 4, 404-418.

Zhao Q., Gregory C.A., Lee R.H., Reger R.L., Qin L., Hai B., Park M.S., Yoon N., Clough B., McNeill E., Prockop D.J. and Liu F. (2015). MSCs derived from iPSCs with a modified protocol are tumor-tropic but have much less potential to promote tumors than bone marrow MSCs. Proc. Natl. Acad. Sci. USA 112, 530-535.

Zhu Y., Wu X., Liang Y., Gu H., Song K., Zou X. and Zhou G. (2016). Repair of cartilage defects in osteoarthritis rats with induced pluripotent stem cell derived chondrocytes. BMC Biotechnol. 16, 78.

Accepted September 22, 2020